Chemometrics and Intelligent Laboratory Systems, 15 (1992) 185–193
Elsevier Science Publishers B.V., Amsterdam

Identification and application of a prognostic vector for use in multivariate calibration and prediction

Rodney P. Williams, Dom A.J. Swinkels and Marcel Maeder
Department of Chemistry, University of Newcastle, Callaghan NSW (Australia)

(Received 3 June 1991; accepted 27 February 1992)

Abstract

Williams, R.P., Swinkels, D.A.J. and Maeder, M., 1992. Identification and application of a prognostic vector for use in multivariate calibration and prediction. *Chemometrics and Intelligent Laboratory Systems*, 15:185–193.

Examination of the mathematical structures of principal components regression and partial least-squares regression has led to the identification of a prognostic vector for both techniques that contains information about the contribution of each feature in a sample spectrum to the quality of the sample. The properties and use of the prognostic vector are demonstrated by a practical application involving the estimation of electrolytic manganese dioxide battery activity from X-ray diffraction patterns. Results from the study suggest that the prognostic vectors derived from both PCR and PLS are similar, and provide information that can ultimately be used to improve sample quality.

INTRODUCTION

In many cases there is a well-defined relationship between some property of interest and the value of an easily accessible measurement. The classical example is the Beer–Lambert law which relates the absorption of a solution at a given wavelength to the concentration of the single solvate via its molar absorptivity at this wavelength. After calibration (determination of the molar absorptivity coefficient) the determination of an unknown concentration in a given solution is trivial.

In many other cases, however, there is no explicitly defined relationship between the value of interest (the sample quality) and some readily available measurement. Principal component regression (PCR) [1,2] and partial least-squares regression (PLS) [3–8] are two recently developed methods based on a 'model-free' approach, which are designed to determine an empirical relationship between the spectrum of a sample and the sample quality. Typical examples are: the prediction of the octane number of gasoline based on measurements in the near-infrared [9]; characterisation of coal and iron ore based on Fourier transform infrared (FT-IR) spectroscopy [10]; and the determination of the battery activity of electrolytic manganese dioxide from X-ray diffraction patterns [11]. Both PCR and PLS are multivariate methods which means that they rely on measurements made on samples using instrumental techniques such as UV–VIS or FT-IR in absorption

Correspondence to: Dr. M. Maeder, Department of Chemistry, University of Newcastle, Callaghan NSW 2303, Australia.

mode, which provide measurements at a large number of channels.

Similar to traditional analytical chemistry techniques, a two-step procedure allows the quantitative prediction of sample quality for unknown samples on the basis of their spectra. The first step involves calibration. For a set of calibration samples, the property of interest and the spectrum of each individual sample has to be determined. The relationship between them is cast into an empirical formula, and its parameters calculated. The second step is prediction, where the formal relationship is used to predict the quality of an unknown sample from its corresponding spectrum.

Analysis of the mathematics used in the PCR and PLS procedures reveals the formal existence of a vector of regression coefficients which is able to reveal the relationship between spectral features of a sample and the sample quality. We suggest calling this vector the 'prognostic vector'. The primarily empirical relationship can be investigated in a further step to lead to a better understanding of the whole problem. The prognostic vector is truly prognostic in nature, as it can be used for both predictive and diagnostic purposes.

Although both procedures have been designed differently, the mathematics on which PCR and PLS are based are very similar. In this contribution we compare the two mathematical structures and apply both methods to a practical example: evaluation of electrolytic manganese dioxide (EMD) battery activity from powder X-ray diffraction patterns. This allows comparison of the prediction capability of the algorithms, as well as the opportunity to demonstrate the properties and use of the prognostic vector.

PCR AND PLS THEORY

The spectra of a set of n_s calibration samples measured at n_c channels (e.g. wavelengths, wavenumbers, etc.), are collected row-wise in the matrix **Y**. The sample quality for each calibration sample is also determined and is collected in the column vector $\boldsymbol{q}$ containing n_s elements. As usual in PLS the data in **Y** and $\boldsymbol{q}$ are column-mean centred prior to calibration [4]. The same mean centred matrices are used in the PCR calculation.

In both PCR and PLS regression, the matrix **Y** is decomposed into a product of smaller matrices. In PCR, this is achieved according to the singular-value decomposition [12]

$$\mathbf{Y} = \mathbf{USV} \tag{1}$$

where the matrices **U**, **S**, and **V** have the following properties: $\mathbf{U}^T\mathbf{U} = \mathbf{V}\mathbf{V}^T = \mathbf{I}$ (**I** is the identity matrix and superscripts T indicates the transposed matrix) and **S** is a diagonal matrix, its diagonal elements corresponding to the singular values of **Y** in decreasing order. In PLS, **Y** is decomposed into a product of two matrices [3–8]

$$\mathbf{Y} = \mathbf{TB} \tag{2}$$

with the property $\mathbf{T}^T\mathbf{T} = \mathbf{I}$.

The singular-value decomposition procedure is well defined, whereas the PLS decomposition is not unique and different authors suggest slightly different procedures for calculating the decomposition $\mathbf{Y} = \mathbf{TB}$. It is not the aim of this contribution to discuss these problems, and we refer the reader to the original literature [3–8,13].

The number of columns in **U** and **T** or rows in **V** and **B** necessary to represent the original matrix **Y** within the limits of measurement noise can be determined using statistical procedures [14]. However, the number which results in an optimal prediction capability for unknown samples might be different, and is best determined using the cross-validation procedure (see later in this text).

The basic principle behind obtaining a calibration model using either method is that the vector $\boldsymbol{q}$, which contains the qualities of all the individual samples in the calibration set, should be a linear combination of the significant columns of **U**, for PCR, or of **T** for PLS. This approximation is readily formulated in terms of a matrix equation

$$\boldsymbol{q} \approx \boldsymbol{q}_{PCR} = \mathbf{U}\boldsymbol{a}_{PCR} \tag{3}$$

and

$$\boldsymbol{q} \approx \boldsymbol{q}_{PLS} = \mathbf{T}\boldsymbol{a}_{PLS} \tag{4}$$

where q_{PCR} and q_{PLS} are the calibration-fitted estimates of q for PCR and PLS, respectively, and a_{PCR} and a_{PLS} are column vectors containing the regression coefficients relating q to the columns of U and of T for PCR and PLS, respectively.

The calibration process for both methods determines those vectors a which optimally represent the actual qualities, q, by the calculated approximations q_{PCR} and q_{PLS}. As a consequence of the orthonormality of U and T, this calculation is straightforward

$$a_{PCR} = \mathbf{U}^T q, \quad q_{PCR} = \mathbf{U}\mathbf{U}^T q \tag{5}$$

and

$$a_{PLS} = \mathbf{T}^T q, \quad q_{PLS} = \mathbf{T}\mathbf{T}^T q \tag{6}$$

Calibration information is contained in a_{PCR} and a_{PLS} and can be used to predict the unknown quality, q_s, of a new sample. Prediction of q_s initially involves projection of the sample spectrum, y_s, into the space U (for PCR) or the space T (for PLS), and is represented by Eqns. 7 and 8, respectively.

$$u_s = y_s \mathbf{V}^T \mathbf{S}^{-1} \tag{7}$$

$$t_s = y_s \mathbf{B}^T (\mathbf{B}\mathbf{B}^T)^{-1} \tag{8}$$

It should be noted that the inversion of $\mathbf{B}\mathbf{B}^T$ can be numerically problematic, with some authors proposing an additional orthogonalisation of B to improve the numerical stability of the algorithm [4].

The predicted quality is then calculated similarly to that shown in Eqns. 3 and 4

$$q_s = u_s a_{PCR} = y_s \mathbf{V}^T \mathbf{S}^{-1} a_{PCR} \quad \text{(for PCR)} \tag{9}$$

$$q_s = t_s a_{PLS} = y_s \mathbf{B}^T (\mathbf{B}\mathbf{B}^T)^{-1} a_{PLS} \quad \text{(for PLS)} \tag{10}$$

Eqns. 9 and 10 can be rewritten as

$$q_s = y_s p_{PCR} \quad \text{(for PCR)} \tag{11}$$

$$q_s = y_s p_{PLS} \quad \text{(for PLS)} \tag{12}$$

where

$$p_{PCR} = \mathbf{V}^T \mathbf{S}^{-1} a_{PCR} \tag{13}$$

$$p_{PLS} = \mathbf{B}^T (\mathbf{B}\mathbf{B}^T)^{-1} a_{PLS} \tag{14}$$

The vectors p are column vectors, and their scalar product with the spectrum, y_s, of the unknown sample yields its quality, q_s. The p vectors are formally regression coefficients, and for the case of PLS it has been identified previously (e.g. vector b in Eqn. 36 in ref. 6). However, the interpretation of this abstract vector of regression coefficients has not been suggested; its explicit calculation is not necessary, and has actually been discouraged [6].

The simple rule for the scalar product of two vectors allows a straightforward interpretation of the prognostic vector p. Unlike the eigenvectors contained in the matrices U and V, or the information contained in the matrices T and B, the prognostic vector is physically interpretable, and contains chemical information relating sample quality to spectral features. The prognostic vector contains all the significant information used in the calibration model construction, and therefore is superior to using other information such as PLS factor 1, which has been suggested for use in qualitative band assignments [13].

A simple demonstration of the properties of the prognostic vector is provided in Fig. 1. Assuming that values measured at each channel of the spectrum are positive, then: (a) a positive

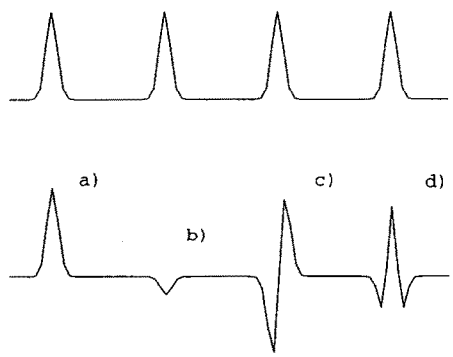

Fig. 1. Relationship between the sample spectrum (upper half) and typical features of the prognostic vector (lower half). See text for details.

feature in the prognostic vector indicates a positive contribution by a sample feature at this position; (b) a small negative feature indicates a small negative contribution; a derivative-like feature (c) indicates that a shift of the signal peak towards the right would be favourable; and a second derivative-type feature (d) indicates a positive effect associated with peak narrowing. A practical example demonstrating the application and interpretation of the prognostic vector is provided below.

PRACTICAL EXAMPLE: THE PREDICTION OF ELECTROLYTIC MANGANESE DIOXIDE BATTERY ACTIVITY FROM POWDER X-RAY DIFFRACTION PATTERNS

EMD is a form of MnO_2 that has been refined by an electrolytic process. It is not a single compound, but may be regarded as a family of closely related, non-stoichiometric compounds, varying slightly both in chemical composition and crystal structure. The type of EMD produced depends on electrolyte temperature, electrolyte composition and current density conditions [15] during electrodeposition. Its crystal structure can be related to a random arrangement of localised domains of several MnO_2 crystal phases. These phases include ramsdellite, γ-MnO_2 (nsutite), ϵ-MnO_2 (fibrous EMD), α-MnO_2 (cryptomelane) and β-MnO_2 (pyrolusite).

EMD is primarily used as a cathodic material for alkaline cells, and must fulfill the criteria of high purity, high battery activity and high charge capacity. Battery activity can be defined as the ability of an EMD to electrochemically reduce under battery discharge conditions. It has been shown in several studies [16,17] that the battery activity of EMD is qualitatively related to the MnO_2 crystal phase composition of the EMD, with EMD samples containing large proportions of γ- and ϵ-MnO_2 having a higher battery activity than samples containing large proportions of β- and α-MnO_2.

Battery activity may be evaluated using an alkaline discharge activity (ADA) test [18]. The total duration of the ADA test, including raw materials preparation and cell discharge, takes approximately two days. The duration of the test represents an unacceptably long delay between the production of the sample and the evaluation of its quality for quality control purposes in a full-scale production plant. Accordingly, researchers in this area have attempted to discover alternate methods that reduce this delay.

Most of the attempts to find rapid methods for EMD battery activity determination have involved use of the powder X-ray diffraction (XRD) pattern of the EMD. XRD is the technique which the battery industry has adopted as the standard method of EMD structure identification, as it provides information pertaining to the MnO_2 crystal phase composition of the EMD. The strong correlation observed between the MnO_2 crystal phase composition of the EMD, and the corresponding EMD battery activity, suggests that quantitative battery activity information exists in the XRD pattern. This has been confirmed [19], and it has been suggested that chemometric techniques could be used to extract quantitative battery activity information from powder XRD patterns.

Data collection

The nineteen EMD samples used in this study belong to the International Battery Materials Association (IBA) common sample series [18]. These samples have been collected over the last twenty years from various EMD manufacturers around the world, and were produced using a large range of process conditions. Correspondingly, a large range in the sample quality is observed within this set, as technological changes have improved EMD manufacturing methods. The use of a global sample set such as this provides a thorough test of the range of applicability of any chemometric method developed.

All samples used were of a similar particle size distribution. XRD patterns of these samples were recorded using a Siemens D-500 X-ray diffractometer with Cu K_α radiation. Counts were accumulated for 10 s, with 2Θ values in the 15–100° range (at 0.1° increments) being extracted to provide 851 data points for the spectra of each

sample. Battery activity values for the samples used in this study were taken from ref. 18, and expressed in terms of RDC20 values, where RDC20 is the relative discharge capacity of an EMD at a constant load of 20 mA relative to a standard sample set to 100.

Data analysis

Calculations were performed by a menu-driven computer program called CHEMTOOL, using TURBO-BASIC as the programming language on an IBM compatible computer. CHEMTOOL was originally developed during this study specifically for use in determining EMD battery activity from the corresponding XRD pattern, but was later adapted for general application to any chemometric problem which requires the prediction of either a concentration or a material property value from instrumental data.

CHEMTOOL gives the user the option to either construct a calibration model or to predict quality values using PCR or PLS. It also has the facility to test the predictability of a PCR or PLS calibration model using cross-validation. The user has the option of using integer, single precision or double precision real data, depending on data type and memory constraints.

Calibration model construction options include data normalisation (both by maximum peak height and area under spectrum), data mean centring (both column and row), factor selection and sample validation. CHEMTOOL also calculates and displays the prognostic vector corresponding to a formulated calibration model.

Calibration model construction

The calibration model construction procedure used in this study was the same for both PCR and PLS, so as to provide a common basis for comparison of both the relative prediction capability and the information contained in the prognostic vector for each technique. For each calibration sample, data were normalised to constant area under the sample spectrum to eliminate differences between the sample spectra due to non-identical sample measurement conditions, e.g. variation in X-ray beam intensity. Calibration spectra and their associated quality values were also mean centred [4,13]. The number of factors required to produce a calibration model with the best prediction capability was calculated using cross-validation.

A full description of cross-validation is provided by Eastment and Krzanowski [20]. Cross-validation involves removing one sample from the calibration set, and producing a calibration model from the remaining samples to predict the quality of the other sample. This process is repeated until every sample in the calibration set has had its quality predicted from the remaining samples. The resulting relationship between cross-validation predicted and actual quality values provides a measure of the prediction capability of the model. Cross-validation is superior to just examining the fit of a calibration model, as the predicted value for each sample using the fitting technique is calculated in part from information that is known from the sample.

In this study, cross-validation results were interpreted using the PRESS (prediction residual error sum of squares) formula as shown in Eqn. 15.

$$\mathrm{PRESS} = \frac{1}{n_s} \sum_{i=1}^{n_s} \left[q(i) - q_{\mathrm{PCR/PLS}}(i) \right]^2 \qquad (15)$$

The calibration model with the minimum PRESS value corresponds to the model with the best prediction capability. For both PCR and PLS, two factors were required to produce the model with the best prediction capability. The minimum PRESS values obtained were 4.29 and 5.11 for PCR and PLS, respectively.

Prediction of EMD battery activity using PCR and PLS

Fig. 2 provides a comparison of cross-validation predicted quality versus actual quality for the PCR and PLS calibration models. The dashed line represents the 45° line, indicative of zero PRESS value, i.e. perfect prediction. Comparison of the two graphs show that the results obtained from both techniques are similar, although the

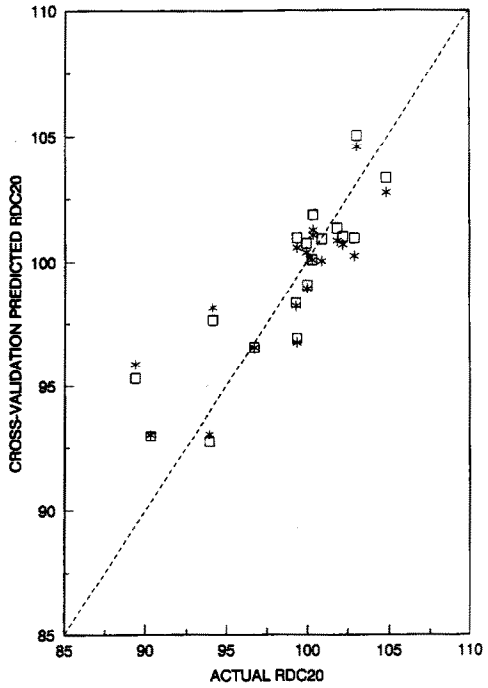

Fig. 2. Cross-validation predicted versus actual RDC20 values for the PCR (□) and PLS (*) methods.

results obtained using the PCR-based calibration model generally lie closer to the zero PRESS line, and suggest that the PCR-model is the better model for prediction of EMD battery activity from the corresponding X-ray diffraction pattern. This is an unusual result in a chemometric context, as it is generally believed that PLS is a superior technique to PCR for prediction of quality from multivariate data [5].

In general, both the PCR- and PLS-based models can be applied to the prediction of EMD battery activity from a global calibration set, with all RDC20 values except one predicted within 3.5% of actual quality values. The prediction error may be due in part to errors in battery activity determination and XRD measurements, as this defines the minimum error that any chemometric technique can predict within. It is expected that improvements in model prediction capability can be achieved by using plant-specific data for calibration and prediction, thereby removing errors created by calibration set samples produced using different methods.

Observation of the results presented in this study have shown that this may particularly be the case for samples with an RDC20 value greater than 100. Ultimately, prediction capability may be limited by the extent of contribution of EMD crystal structure to battery activity, as other battery activity related sample properties are not being considered in the model.

Chemical information contained in the prognostic vector

The prognostic vectors corresponding to the PCR and PLS calibration models are presented in Fig. 3. Comparison of the two spectra shows that the prognostic vectors are very similar in shape and contain similar features in the same 2Θ locations. Closer examination shows that there are differences between the two prognostic vec-

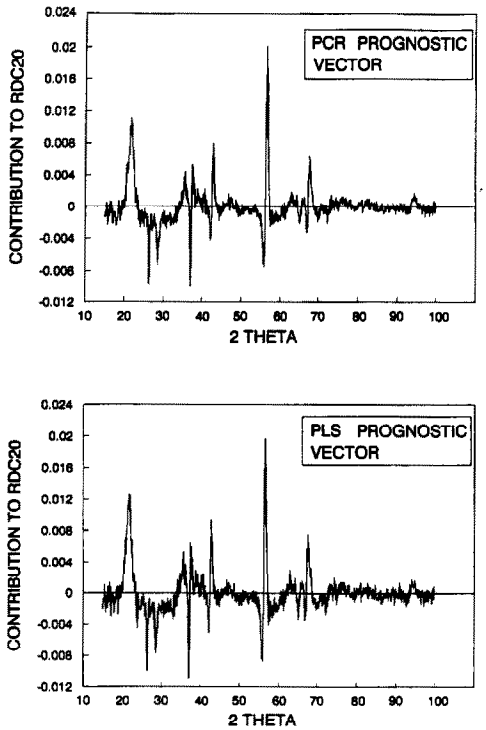

Fig. 3. The prognostic vectors for PCR and PLS.

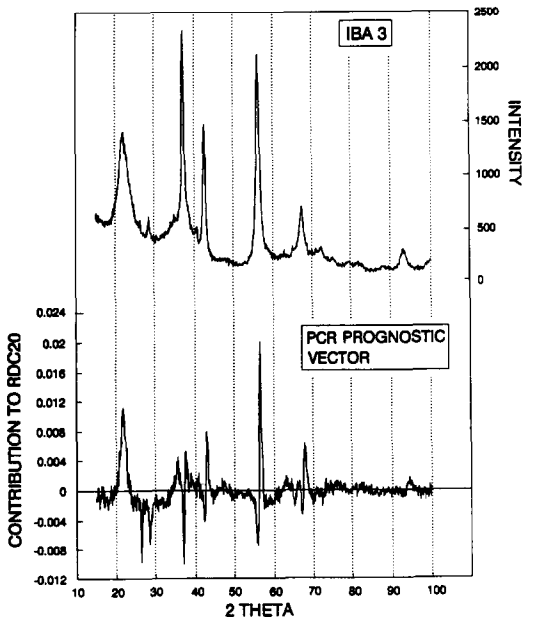

Fig. 4. The relationship between the XRD of an EMD sample and the PCR prognostic vector.

tors with respect to the relative heights of corresponding peaks. For example, the ratio of the peak at 22.2° 2Θ to the peak at 56.7° 2Θ in the PLS prognostic vector is greater than the corresponding ratio in the PCR prognostic vector, and shows that the different methods assign slightly more importance to some features than to others. These slight differences account for the differences observed in the predicted quality values obtained using the two methods.

The properties of the prognostic vector make it very useful for analysing areas in a spectrum which have an influence on quality values, and can therefore provide information which can be used to improve sample quality. An example of this is provided in Fig. 4, which represents a comparison between the powder XRD pattern of one of the samples used in this study, IBA 3, and the prognostic vector derived from the PCR-based calibration model.

From Fig. 4, it can be seen that the position of the largest variations in the contribution to battery activity correspond to XRD peaks, and hence to EMD crystal phase composition. The prognostic vector indicates that the γ-MnO_2 peak at 22.2° 2Θ makes a positive contribution to battery activity, whereas the β-MnO_2 peak at 28.6 2Θ contributes negatively to battery activity. These observations confirm the qualitative relationship between MnO_2 crystal phase and EMD battery activity discussed earlier in the paper. The prognostic vector also indicates that an improvement in quality would be obtained if the peak at 37.3° 2Θ was broadened due to the emergence of additional γ-MnO_2 peaks at 34.6° and 38.6° 2Θ [21], and the peaks at 42.8, 56.7 and 67.6° 2Θ, which are common to many MnO_2 phases, were shifted to slightly higher 2Θ values. This observation suggests that the battery activity of EMD can be improved if the average spacing between certain crystal layers of MnO_2 is slightly decreased.

Another feature of the prognostic vector is the large negative contribution to battery activity associated with the small graphite peak at 26.5° 2Θ. The graphite is present in the sample as IBA 3 was produced using a graphite anode. The negative contribution corresponding to the graphite peak suggests that there is a reduction in the battery activity of EMD samples produced using graphite anodes as opposed to those produced using titanium anodes, because electrolysis conditions normally used on graphite electrodes were not as favourable to battery activity as those used on titanium anodes.

CONCLUSION

Results from this study have shown that both PCR and PLS can be used to derive a prognostic vector that contains information regarding contribution to sample quality at each channel in a spectrum produced from that sample. This enables information that can be interpreted and used to improve sample quality to be readily gained by examining the contribution to sample quality associated with every peak in a sample spectrum.

PCR and PLS were compared using a practical example: evaluation of EMD battery activity from powder XRD patterns, so as to determine whether one technique provided a better predic-

tion capability and more chemical information related to sample quality than the other. A comparison of the results obtained from the two techniques suggests that results produced using a PCR-based calibration model were slightly better than those produced using a PLS-based calibration model. The relatively poor prediction results obtained using both PCR and PLS can be attributed to the large differences in the samples associated with their global nature, and can be expected to improve with the use of plant and/or process specific data.

Comparison of the corresponding prognostic vectors produced from the PCR- and PLS-based calibration models also shows that both are very similar, each containing similar features at locations that correspond to features in the EMD powder XRD pattern. It was also shown that both prognostic vectors can be used to obtain chemical information that indicates aspects of EMD structure and production methods that can lead to an improvement in EMD quality.

Obviously, in this paper, the discussion of the features of the PCR and PLS prognostic vectors and their relative similarities is related to our specific example of EMD. Only future investigations and applications in a variety of different cases will reveal a more general picture of the applicability and value of the prognostic vector.

REFERENCES

1 I.T. Jolliffe, *Principal Component Analysis*, Springer-Verlag, New York, 1986.

2 P.M. Fredericks, J.B. Lee, P.R. Osborn and D.A.J. Swinkels, Materials characterisation using factor analysis of FT-IR spectra. Part 2: mathematical and statistical considerations, *Journal of Applied Spectroscopy*, 39 (1985) 311–316.

3 S. Wold, M. Sjöström, W. Lindberg, J.-A. Persson and H. Martens, A multivariate calibration problem in analytical chemistry solved by partial least-squares models in latent variables, *Analytical Chimica Acta*, 150 (1983) 61–70.

4 P. Geladi and B.R. Kowalski, Partial least-squares regression: a tutorial, *Analytical Chimica Acta*, 185 (1986) 1–17.

5 A. Lorber, L.E. Wangen and B.R. Kowalski, A theoretical foundation for the PLS algorithm, *Journal of Chemometrics*, 1 (1987) 19–31.

6 R. Manne, Analysis of two partial-least-squares algorithms for multivariate calibration, *Chemometrics and Intelligent Laboratory Systems*, 2 (1987) 187–197.

7 A. Höskuldsson, PLS regression methods, *Journal of Chemometrics*, 2 (1988) 211–228.

8 E. Sanchez and B.R. Kowalski, Tensorial calibration. 1. First-order calibration, *Journal of Chemometrics*, 2 (1988) 267–263.

9 J.J. Kelly, C.H. Barlow, T.M. Jinguji and J.B. Callis, Prediction of gasoline octane numbers from near infrared spectral features in the range 660–1250 nm, *Analytical Chemistry*, 61 (1989) 313–320.

10 P.M. Fredericks, J.B. Lee, P.R. Osborn and D.A.J. Swinkels, Materials characterisation using factor analysis of FT-IR spectra. Part 1: results, *Journal of Applied Spectroscopy*, 39 (1985) 303–310.

11 R.P. Williams, D.A.J. Swinkels and M. Maeder, Principal components regression in practice: an evaluation of EMD battery activity from X-ray diffraction patterns, *Trends in Analytical Chemistry*, 9 (1990) 303–308.

12 G.H. Golub and F. Van Loan, *Matrix Computations*, John Hopkins University Press, Baltimore, MD, 1983.

13 D.M. Haaland and E.V. Thomas, Partial least squares methods for spectral analysis. 1. Relation to other quantitative calibration methods and the extraction of qualitative information, *Analytical Chemistry*, 60 (1988) 1193–1202.

14 E.R. Malinowski, Statistical F-tests for abstract factor analysis and target testing, *Journal of Chemometrics*, 3 (1988) 49–60.

15 E. Voss, H. Laig-Horstebrock, W. Krey, H.W. Nientiedt, A. Winsel, E. Preisler, O. Glemser and Th. Pfeiffer, Recovery of zinc, manganese (MnO_2) and mercury from Leclanché and alkaline manganese dioxide cells, *Varta Battery AG, Final Report, Project No. RNF-002-D*, Varta Battery AG, Ellwangen, 1983–1986.

16 P. Ruetschi, Cation-vacancy model for MnO_2, *Journal of the Electrochemical Society*, 131 (1984) 2737–2744.

17 E. Preisler and G. Mietens, Effects of the properties of electrolyte manganese dioxide on the discharge dynamics of alkaline cells, *Dechema-Monographien*, 109 (1987) 123–137.

18 S.F. Burkhardt, *Handbook of Manganese Dioxides*, IBA Inc., Brunswick, OH, 1989.

19 D.A.J. Swinkels, Chemometric treatment of XRD patterns, *Progress in Batteries and Solar Cells*, JEC Press, Brunswick, OH, 1990, pp. 9–20.

20 H.T. Eastment and W.J. Krzanowski, Cross-validatory choice of the number of components from a principal components analysis, *Technometrics*, 24 (1982) 73–77.

21 D.G. Malpas and F.L. Tye, *Handbook of Manganese Dioxides*, IBA Inc., Brunswick, OH, 1989.

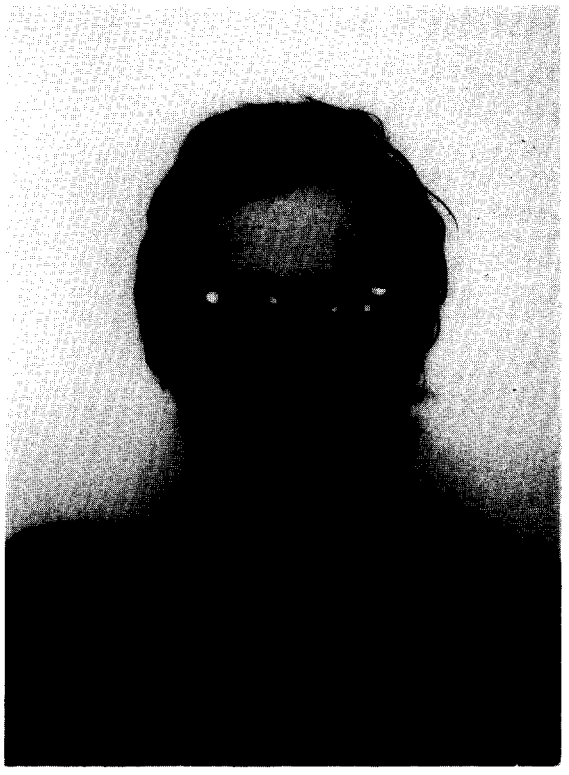

BIOGRAPHICAL SKETCH

Marcel Maeder did his undergraduate studies and his Ph.D. at the University of Basel. After a post-doctoral at the Research School of Chemistry of the Australian National University in Canberra he went back to Basel to do a Habilitation. Since 1988 he is in the Department of Chemistry at the University of Newcastle in Australia.